PAPER

Check for updates

Peroxomolybdate@MOFs as effective catalysts for oxidative desulfurization of fuels: correlation between MOF structure and catalytic activity

Yan Gao,[ab] Carlos M. Granadeiro, [iD][a] Luís Cunha-Silva, [iD][b]
Jianshe Zhao [iD] *[b] and Salete S. Balula [iD] *[a]

The highly active peroxomolybdate, $TBA_3\{PO_4[MoO(O_2)_2]_4\}\cdot 3H_2O$ (abbreviated as PMo_4), was incorporated for the first time in various porous MOF support structures (MIL-101, MOF-808, and ZIF-8) to form heterogeneous catalysts with different structural properties. These catalysts were used to treat a multicomponent model diesel *via* an oxidative desulfurization process. Sulfur-free diesel could be obtained after only 2 h depending on the porous MOF structural morphology. The size of the window entrance and the dimension of the pore from the MOF support had a remarkable influence on the catalytic performance of $PMo_4@MOF$ catalysts, and thus, the conditioning of reactant diffusion. $PMo_4@MIL$-101 presented the highest catalytic efficiency (100% after 2 h), followed by $PMo_4@MOF$-808 (73.1% at 2 h) and $PMo_4@ZIF$-8 (68.1% at 2 h). Furthermore, the most active catalyst, $PMo_4@MIL$-101, showed remarkable recycle capacity and structural stability (maintaining the activity and stability for 10 catalytic cycles). Appropriate window and pore size cavities from MIL-101 support were the most suitable for organosulfur oxidation. Smaller windows and pore sizes from the other MOFs caused a decrease in catalytic efficiency. The windows and porous dimensions from MOF-based catalysts have a direct effect on catalyst performance, and these must be adjusted to reactants and active guest centers to avoid leaching and allow a fluent diffusion of reactants, mainly the ones with large molecular sizes.

1. Introduction

Fossil fuel combustion still accounts for ~85% of the world's energy production and the goal for 2040 is to decrease this to 20%.[1,2] Therefore, crude oil is and will be the principal energy source for the chemical industry, transportation, and other human activities. Sulfur compounds form one of the major impurities present in crude oil, which are responsible for acid rains that cause a series of environmental and human health problems.[3] Of the various sulfur compounds present in crude oil, organosulfur species are the most important. Sulfur present in fossil fuels can be higher than 35 000 ppm. Consequently, legislation has been implemented to limit sulfur concentration in commercial road and maritime fuels, whereby maximum sulfur concentration in road diesel is limited to 10 ppm;[4] more recently, in marine fuels, it has been limited to 500 ppm (100

ppm in the Baltic Sea, North Sea, and the English Channel) by the International Marine Organization.[5] The efficiency of the current industrial hydrodesulfurization process is limited to some liquid fuels (gasoline and diesel) and must use more severe conditions (higher temperature and hydrogen pressure) to achieve 10 ppm of sulfur content. Therefore, the desulfurization of fuels is still a hot research topic that aims to develop effective processes to treat fuels mainly containing high-molecular-weight aromatic sulfur compounds.[6,7] Various examples are reported using alternative desulfurization processes, such as oxidation, adsorption, extraction, and biodegradation technologies.[8-13] Among these alternative methods, oxidative desulfurization is becoming a dominant technique to remove organosulfur compounds *via* oxidation to prepare ultra-low sulfur fuels under moderate experimental conditions.[12,14-27] In an oxidative catalytic desulfurization system, the organosulfur compounds are oxidized to sulfoxide and/or sulfones, which are easily removed by extraction using an immiscible polar solvent. Another possibility for oxidative desulfurization is based on performing simultaneous extraction and oxidation catalytic processes using a biphasic system comprising fuel and an immiscible polar solvent (extractive/catalytic oxidative desulfurization system, ECODS). In this case, this polar solvent presents a double functionality of receiving

[a] REQUIMTE/LAQV & Department of Chemistry and Biochemistry, Faculty of Sciences, University of Porto, 4169-007 Porto, Portugal. E-mail: sbalula@fc.up.pt
[b] Key Laboratory of Synthetic and Natural Functional Molecule Chemistry of Ministry of Education, Shaanxi Key Laboratory of Physico-Inorganic Chemistry, College of Chemistry & Material Science, Northwest University, Xi'an, Shaanxi 710127, China. E-mail: jszhao@nwu.edu.cn

This journal is © The Royal Society of Chemistry 2023

Catal. Sci. Technol., 2023, **13**, 4785–4801 | **4785**

the organosulfur compounds from the fuel phase and promoting a suitable medium for efficient oxidative catalysis.[28–32] The strategic combination of a highly efficient catalyst and a sustainable extraction medium is needed to achieve deep desulfurization in a short period of time. Hydrogen peroxide has been demonstrated to be an effective oxidant for oxidative desulfurization processes that are catalyzed by polyoxometalates and are considered to produce no harmful by-products.[16,18,22–25,29,33–40] POMs have proved to be an extraordinary class of catalysts with exceptional reactivity for ODS of fuels that use H_2O_2 as an oxidant.[18,22–25,27,41–45] POMs are a class of highly ordered well-defined nanometer-sized inorganic cluster ionic compounds, normally presenting high solubility in various reaction media dependent on the nature of the counter-cation. Therefore, various strategic paths have been investigated to heterogenize POM units on solid supports, which should promote their stability and maintain their homogeneous catalytic activity. Amongst the several solid supports available, porous metal–organic frameworks (MOFs) feature important advantages over traditional inorganic and organic solid supports, such as ordered pore structure and suitable pore size that promotes uniform incorporation of POM units.[46–50] The regular distribution of POMs within the MOF cavities can be enforced by easy pre-structural functionalization of the MOF structure. This procedure avoids POMs agglomeration and deactivation.[49,51–53] In general, two main experimental methodologies have been applied in the preparation of the POM@MOF composite materials: the impregnation method and the one-pot approach, frequently named "bottle-around-the-ship". Various examples are reported in the literature presenting POM@MOF composites as heterogeneous catalysts for oxidative desulfurization systems.[2,54–62] The mechanism involved in oxidative desulfurization processes catalyzed by POMs is attributed to the generation of peroxopolyoxometalates (POOMs) as the active catalytic centers, where POOMs are formed by the interaction of the POM precursor and the H_2O_2 oxidant.[2,63–66] However, active POOMs lack good recyclability and reusability due to their homogeneous nature which promotes high solubility in organic solvents. Therefore, it is essential to investigate procedures for the effective heterogenization of active POOMs; however, the work reported in this area is scarce.[2,40] Our research group recently reported the immobilization of a peroxopolyoxotungstate, $(nBu_4N)_3\{PO_4[WO(O_2)_2]_4\}$ (PW$_4$) on the surface of a functionalized mesoporous SBA-15 support[40] and also its encapsulation in a MOF structure with large pore cavities (MIL-101).[2] Porous MOFs have the advantage of acting as nanoreactors for liquid phase catalytic systems; however, the size of their pore window and pore cavity must be adjusted to the catalytic active center to avoid its leaching and deactivation during the recycling processes.

Following our recent report on the encapsulation of a peroxopolyoxotungstate in the MOF, MIL-101, with large pore cavities,[2] the highly active peroxophosphomolybdate with Venturello structure, $(nBu_4N)_3\{PO_4[MoO(O_2)_2]_4\}$ (hereafter abbreviated as PMo$_4$),[17] was incorporated into three distinct

MOFs (ZIF-8, MOF-808, and MIL-101) with diverse cavities/window dimensions. These composites were used as catalysts for the oxidative desulfurization of a multi-component diesel. The correlations between activity and structural features of the porous MOF supports were studied and discussed. In fact, the application of peroxomolybdate-based heterogeneous catalysts for the oxidative desulfurization of model fuels is herein reported for the first time. Interestingly, despite the structural similarity of both PMo$_4$ and PW$_4$, the peroxotungstate revealed the superior homogeneous catalytic performance in the oxidative desulfurization of model fuels.[64] However, the heterogeneous catalyst based on the peroxopolyoxomolybdate, PMo$_4$@MIL-101, investigated herein presented enhanced performance than the analogous PW$_4$@MIL-101 that had been previously reported. Furthermore, higher structural stability and recycling ability were found in this work using the heterogeneous PMo$_4$@MIL-101.[2]

2. Experimental section

2.1. Materials and methods

The reagents applied in the synthesis of the materials and used in desulfurization studies were utilized as received without further purification: phosphomolybdic acid hydrate (H_3PMo_{12}-$O_{40}\cdot nH_2O$, PMo$_{12}$, 99.9%, Sigma-Aldrich), tetrabutylammonium chloride (TBACl, 98%, Sigma-Aldrich), hydrogen peroxide (H_2O_2, 30% w/w aq. Sigma-Aldrich), zirconium tetrachloride (ZrCl$_4$, 99.5%, Aldrich), benzene-1,3,5-tricarboxylic acid (trimesic acid, $C_9H_6O_6$ H$_3$btc, 98%, Aldrich), zinc nitrate hexahydrate (Zn(NO)$_3\cdot6H_2O$, 99.0%, Sigma-Aldrich), 2-methylimidazole ($C_4H_6N_2$, 99%, Sigma-Aldrich), chromium(III) nitrate nonahydrate (Cr(NO)$_3\cdot9H_2O$, 99%, Aldrich), benzene-1,4-dicarboxylic acid (terephthalic acid, $C_8H_6O_4$, H$_2$bdc, 98%, Aldrich), hydrofluoric acid (HF, 40–45%, Aldrich), acetic acid (CH$_3$COOH, 99%, Sigma-Aldrich), 1-benzothiophene (1-BT, Fluka), dibenzothiophene (DBT, Aldrich); 4-methyldibenzothiophene (4-MDBT, Aldrich), 4,6-dimethyldibenzothiophene (4,6-DMDBT, Alfa Aesar), decane (98%), tetradecane (99%), 1-butyl-3-methylimidazolium hexafluorophosphate ([BMIM]PF$_6$, Aldrich, 99%), polyethylene glycol (PEG, Sigma-Aldrich, BioUltra 200), and acetonitrile (MeCN, Sigma-Aldrich 99%).

Elemental analysis for C, H, and N was performed on a Leco CHNS-932 instrument to confirm the structural formula of PMo$_4$. The content of metal elements, Mo and Cr, was determined by ICP-OES on a Perkin-Elmer Optima 4300 DV instrument. FT-IR spectra were recorded on a Jasco 460 Plus spectrometer with 64 scans in the region of 1800–400 cm^{-1}. Powder XRD patterns were recorded in the 2–50° range on an X'Pert MPD Philips diffractometer with a scanning speed of 0.1° min^{-1} at 45 kV and 40 mA. Scanning electron microscopy (SEM) images were acquired on a JEOL JSM 6301F microscope using a 15 kV acceleration voltage equipped with an Oxford INCA Energy 350 energy-dispersive X-ray spectrometer at "Centro de Materiais da Universidade do Porto" (CEMUP, Porto, Portugal). Thermogravimetric analysis

4786 | *Catal. Sci. Technol.*, 2023, **13**, 4785–4801

This journal is © The Royal Society of Chemistry 2023

was carried out in a nitrogen atmosphere on a STA7200RV equipment at a heating rate of 5 °C min^{-1}. These analyses were performed to test the stability of the materials from 30 to 1000 °C under a nitrogen atmosphere with a temperature increase at a rate of 5 °C min^{-1}. N_2 adsorption–desorption isotherms were collected at −196 °C with a gas porosimeter Micromeritics ASAP 2010. Pre-outgassing of the analyzed samples was carried out at 150 °C for 2 h. The concentration of sulfur-containing substances was monitored by GC-FID analysis on Bruker 430-GC-FID chromatograph equipped with fused silica Supel-Co capillary columns SPB-5.

2.2. Catalysts syntheses

2.2.1. Peroxophosphomolybdate.

$TBA_3\{PO_4[MoO(O_2)_2]_4\}\cdot3H_2O$ (abbreviated as PMo_4) was prepared following published procedures with minor changes.[2] Briefly, aqueous H_2O_2 30% (10 mL, 98 mmol) was slowly dropped into an aqueous solution (10 mL) containing $H_3PMo_{12}O_{40}\cdot nH_2O$ (0.91 g, 0.50 mmol) under magnetic stirring for 60 min. Then, a solution of TBACl (0.45 g, 1.60 mmol) in deionized water (3 mL) was added dropwise into the mixture with vigorous stirring, and a yellow precipitate was generated during this process. The precipitate was collected by vacuum filtration, washed with deionized water, and dried at room temperature. The successful preparation of PMo_4 was confirmed by ^{31}P NMR, FT-IR, and elemental analysis. ^{31}P NMR (161.9 MHz, CD_3CN, 25 °C) presented δ = 8.23 ppm. FT-IR (cm^{-1}) featured peaks at 2960 (w, $v_{asym}(CH_3)$), 2874 (w, $v_{asym}(CH_2)$), 1485 (m, $v(C-N)$), 1070 (vs, $v(PO_4)$), 1039 (s, $v(PO_4)$), 961 (vs, $v(Mo=O)$), 867 (vs, $v(O-O)$), 588 (s, $v_{asym}[Mo(O_2)]$), and 543 (s, $v_{sym}[Mo(O_2)]$). Elemental analysis (%) of $TBA_3\{PO_4[MoO(O_2)_2]_4\}\cdot3H_2O$ (1580.25) calculated C = 36.28, H = 6.93, and N = 2.61 and found: C = 36.48, H = 7.27, and N = 2.66.

2.2.2. MOFs as support materials

ZIF-8. The porous ZIF-8 was synthesized by a method similar to that reported in the literature.[67] 2-methylimidazole (0.82 g, 0.01 mol) was dissolved in MeOH (25 mL) and then injected into a solution of $Zn(NO_3)_2\cdot6H_2O$ (0.74 g, 2.5 mmol) in MeOH (25 mL) with magnetic stirring at room temperature. After stirring for 24 h, a white product was recovered by centrifugation and washed thrice with MeOH. Selected FT-IR (cm^{-1}) was performed for: 1301(w), 1179(w), 1144(s), 994(w), 758(s), 692(w), 680(w), and 419(s).

MOF-808. Porous MOF-808 was prepared by a solvothermal method similar to that already described.[68] A mixture of $ZrCl_4$ (0.93 g, 4 mmol), H_3btc (0.28 g, 1.24 mmol), acetic acid (24 mL, 0.42 mol), and DMF (40 mL, 0.52 mol) was treated by ultrasound to obtain a transparent solution, which was transferred to a Teflon-lined autoclave and heated at 130 °C for 48 h in an electric oven. A white solid was recovered by centrifugation and further washed with DMF and acetone (three washes). Selected FT-IR (cm^{-1}) was performed for: 1656(w), 1620(w), 1570(w), 1445(s), 1379(s), 1078(w), 1047(w), 755(w), 719(w), 651(w), and 448(w).

MIL-101. Porous MIL-101 was synthesized by a reported solvothermal method[69] as follows: $Cr(NO_3)_3\cdot9H_2O$ (0.40 g,

1.00 mmol), H_2bdc (0.166 g, 1.00 mmol), and hydrofluoric acid (100 μL) were added into H_2O (10 mL) and stirred for 10 min at room temperature; the mixture was then transferred to a Teflon reactor and heated at 493 K for 9 h using an electric oven. After the reaction finished, the bottle-green product was isolated by filtration, washed with DMF and MeOH, and dried appropriately. Selected FT-IR (cm^{-1}) was performed for: 1667(w), 1628(w), 1545(w), 1507(w), 1399(s), 1084(w), 1018(w), 972(w), 884(w), 835(w), 745(m), 658(w), and 583(m).

2.2.3. Composite PMo_4@MOFs.

PMo_4@ZIF-8. The incorporation of PMo_4 in ZIF-8 was carried out with a procedure identical to that for ZIF-8, except a solution of PMo_4 (77.3 mg, 0.04 mmol) in DMF (3 mL) was poured into the mixture during the synthesis of ZIF-8. After the reaction, the white solid was separated by centrifugation and washed with DMF and MeOH (thrice). The loading amount of PMo_4 determined by ICP-OES analysis was 0.13 mmol g^{-1}. Selected FT-IR (cm^{-1}) was performed for: 1301(w), 1179(w), 1144(s), 994(w), 758(s), 692(w), 680(w), and 419(s).

PMo_4@MOF-808. The encapsulation of PMo_4 in MOF-808 was performed with a procedure similar to that for MOF-808, which was just the addition of PMo_4 (0.12 mmol) during the synthetic process. The loading quantity of PMo_4 evaluated by ICP-MS analysis was 0.17 mmol g^{-1}. FT-IR (cm^{-1}) analysis: 1656(w), 1620(w), 1570(w), 1445(s), 1379(s), 758(w), 719(w), 651(w), and 448(w).

PMo_4@MIL-101. The insertion of PMo_4 in the cavities of porous MIL-101 was executed *via* an impregnation method: PMo_4 (0.27 g, 0.14 mmol) was dissolved in MeCN (10 mL). Porous MIL-101 (0.44 g) that had been previously dried and activated under vacuum for 12 h at 60 °C, was transferred into the solution and stirred at room temperature (72 hours). The solid material (PMo_4@MIL-101) was recovered by filtration, washed with MeCN and EtOH three times, and dried. The loading amount of PMo_4 calculated by ICP-MS analysis was 0.38 mmol g^{-1}. FT-IR (cm^{-1}) was performed: 1667(w), 1628(s), 1545(w), 1507(w), 1399(s), 1084(w), 1018(w), 972(w), 884(w), 835(w), 745(m), 658(w), and 583(m).

2.3. Desulfurization studies

A multicomponent model diesel with equal concentrations (with a total sulfur concentration of 2000 ppm) of 1-BT, DBT, 4-MDBT, and 4,6-DMDBT was prepared in decane to simulate model diesel. In a typical desulfurization run, two liquid-phases with equal volumes of model diesel and extraction solvent (MeCN, [BMIM]PF$_6$, or TBACl/PEG) were adopted. Desulfurization was performed by the following procedure: a homogeneous catalyst, such as PMo_4 (5 μmol), or a heterogeneous catalyst, such as PMo_4@MOF (containing an equivalent amount of 5 μmol of PMo_4), model diesel (0.75 mL, containing a total of 31 μmol of sulfur), and extraction solvent (0.75 mL) were added into a 5 mL closed borosilicate reactor with magnetic stirring; the mixture was immersed in an oil bath at 70 °C. After 10 min, H_2O_2 (0.26 mmol) was

This journal is © The Royal Society of Chemistry 2023

Catal. Sci. Technol., 2023, **13**, 4785–4801 | 4787

added to the mixture as the oxidant to initiate the oxidative catalytic desulfurization step. The model diesel was then withdrawn from the upper phase (20 μL) and analyzed with the addition of tetradecane as the standard by gas chromatography to quantify the total sulfur content. Finally, the desulfurization efficiency (%) was calculated according to the following formula.

$$\text{Desulfurization efficiency (\%)}$$
$$= \frac{\text{Initial sulfur content} - \text{Residual sulfur content}}{\text{Initial sulfur content}} \times 100\%.$$

The error associated with at least three reproduced experiments was 3% of the total desulfurization. Reusability of homogeneous and heterogeneous catalytic systems was carried out for 10 consecutive desulfurization cycles under optimized conditions: PMo_4 (7.5 μmol) or PMo_4@MIL-101 (an equivalent amount containing 7.5 μmol of PMo_4), model diesel (0.75 mL), [BMIM]PF_6 (0.75 mL), and H_2O_2 (0.78 mmol). After each cycle, desulfurized diesel was removed and an equal amount of fresh untreated model diesel and oxidant were added to initiate the next cycle. The recyclability of heterogeneous catalysts was also evaluated by separating the solid catalyst after each cycle. The catalyst was washed with MeCN, dried, and then poured into a new reactor with fresh untreated diesel and [BMIM]PF_6 to start a new cycle in the presence of H_2O_2.
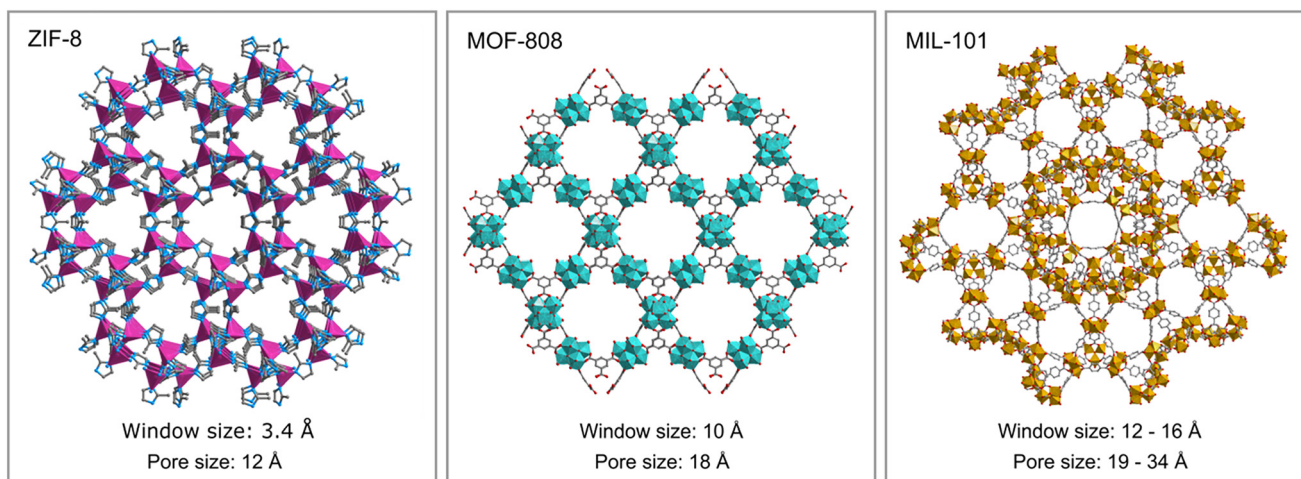
3. Results and discussion

3.1. Structural characterization of materials

The encapsulation of PMo_4 in the different MOFs was attained *via* adequate approaches according to the structural features of each MOF, specifically the pore and aperture (window) sizes in each porous material (Scheme 1). The main challenge was that the cavity should accommodate the soluble PMo_4 to ma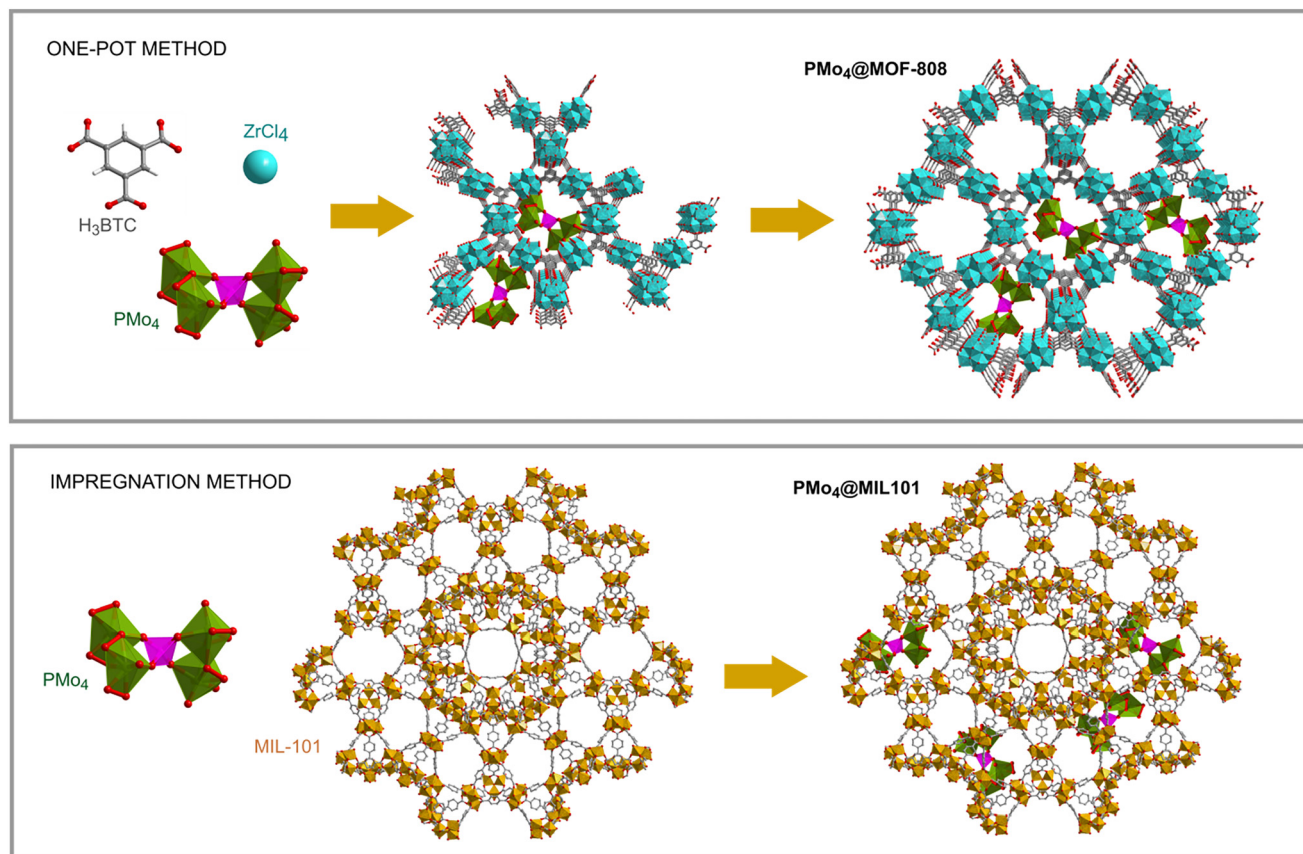intain high catalytic activity, while avoiding their leaching when used as heterogeneous catalysts. PMo_4 can be easily encapsulated in MIL-101 with a larger window size *via* the facile impregnation method. However, due to the small window size of MOF-808 and ZIF-8, the PMo_4 needs to be encapsulated by a one-pot procedure (Scheme 2).

The prepared composites, PMo_4@ZIF-8, PMo_4@MOF-808, and PMo_4@MIL-101, were characterized by a myriad of complementary methods, where they were always compared with the respective pristine MOF using several methods: inductively coupled plasma-OES spectrometer (ICP-OES), Fourier transform-infrared spectroscopy (FT-IR), powder X-ray diffraction (PXRD), scanning electron microscopy (SEM), energy dispersive X-ray spectroscopy (EDX), thermogravimetric analysis (TGA), and N_2 adsorption–desorption studies. Functional groups and relevant structural information on the PMo_4, pristine MOFs, and the different composites were confirmed by FT-IR (Fig. 1). The results showed that practically all the vibrational bands of the pristine MOFs were still present in the spectra of the PMo_4@MOFs composites, suggesting that the MOF structure is preserved after the incorporation procedure. However, the main characteristic bands assigned to PMo_4 were located at 871, 962, 1036, and 1067 cm^{-1} and were not visible in the spectra of PMo_4@MOFs, most likely due to the small relative content of PMo_4 when compared with the amount of MOF. Nevertheless, ICP-OES analysis confirmed the presence of the peroxophosphomolybdate in all composites, leading to a PMo_4 loading of 0.13, 0.17, and 0.38 mmol g^{-1} for PMo_4@ZIF-8, PMo_4@MOF-808, and PMo_4@MIL-101(Cr), respectively. The phase purity of robust MOFs and their respective PMo_4-containing composites was analyzed by powder XRD analysis (Fig. 1). The XRD patterns of pure MOFs were consistent with the simulated and experimental patterns that have been reported in the literature.[70–72] Moreover, the XRD patterns of composites PMo_4@MOFs were similar to the corresponding isolated support material and

Scheme 1 The structural information from selected MOFs.

4788 | *Catal. Sci. Technol.*, 2023, **13**, 4785–4801

This journal is © The Royal Society of Chemistry 2023

Scheme 2 Representation of the two distinct experimental procedures applied for the preparation of the composite materials: one-pot method (used for the preparation of PMo$_4$@MOF-808, top, and PMo$_4$@ZIF-8) and the impregnation method (used to prepare PMo$_4$@MIL-101, bottom).

no additional peaks were found. These results confirm that the structures of supporting MOFs were maintained after introducing the PMo$_4$ guest molecule and that the PMo$_4$ active center was uniformly dispersed within the porous MOFs.

The SEM image of PMo$_4$ showed that the particles of this peroxophosphomolybdate presented an irregular lamellar morphology (Fig. 2). Comparing SEM images of the pristine ZIF-8 and its composite demonstrated that the dodecahedral crystal structure of ZIF-8 was preserved well after encapsulation of the guest PMo$_4$. In addition, the composites, PMo$_4$@MOF-808 and PMo$_4$@MIL-101, also maintained the typical octahedral shape as the original support materials. The similar morphology before and after the incorporation of PMo$_4$, combined with XRD results, indicated that the crystalline structure of selected MOFs was stable and was not destroyed during the incorporation process. In addition, the EDX spectra (Fig. 2) also showed the presence of Mo element arising from PMo$_4$, which further confirmed that the PMo$_4$ was embedded in the MOFs framework.

The thermal stability of all materials was investigated by TG measurements (Fig. 3). The TG curve of pristine PMo$_4$ showed that three crystal waters were lost before 190 °C. Afterward, the decomposition of the tetrabutylammonium cation and the anion of PMo$_4$ occurred from 190 to 412 °C.

The total mass loss was 49.6%, and it can be inferred that the final products were MoO$_3$ and P$_2$O$_5$. The trends of the variations in the catalyst mass of MOFs and the corresponding PMo$_4$-containing composites were similar, and all prepared composites were stable at the temperature of the desulfurization test (70 °C).

The textural properties, including specific surface area, pore size, and pore volume, were obtained through the Brunauer–Emmett–Teller (BET) method (Fig. 4 and Table 1). The N$_2$ adsorption isotherms of the isolated MOFs were in good agreement with previously reported data, with the results exhibiting type I isotherms for ZIF-8 and MOF-808, and type I with minor type IV features for MIL-101(Cr).[73–75] The PMo$_4$@MOFs composites maintained the shape of the adsorption isotherms of the initial MOF support. The PMo$_4$@MIL-101(Cr), prepared by the impregnation method, and the PMo$_4$@ZIF-8 and PMo$_4$@MOF-808, prepared by the *in situ* method, showed a smaller specific surface area owing to the occupation of PMo$_4$ in the respective porous channels or cavities.

3.2. Desulfurization studies

The performance of the desulfurization systems was evaluated using a multicomponent model diesel composed
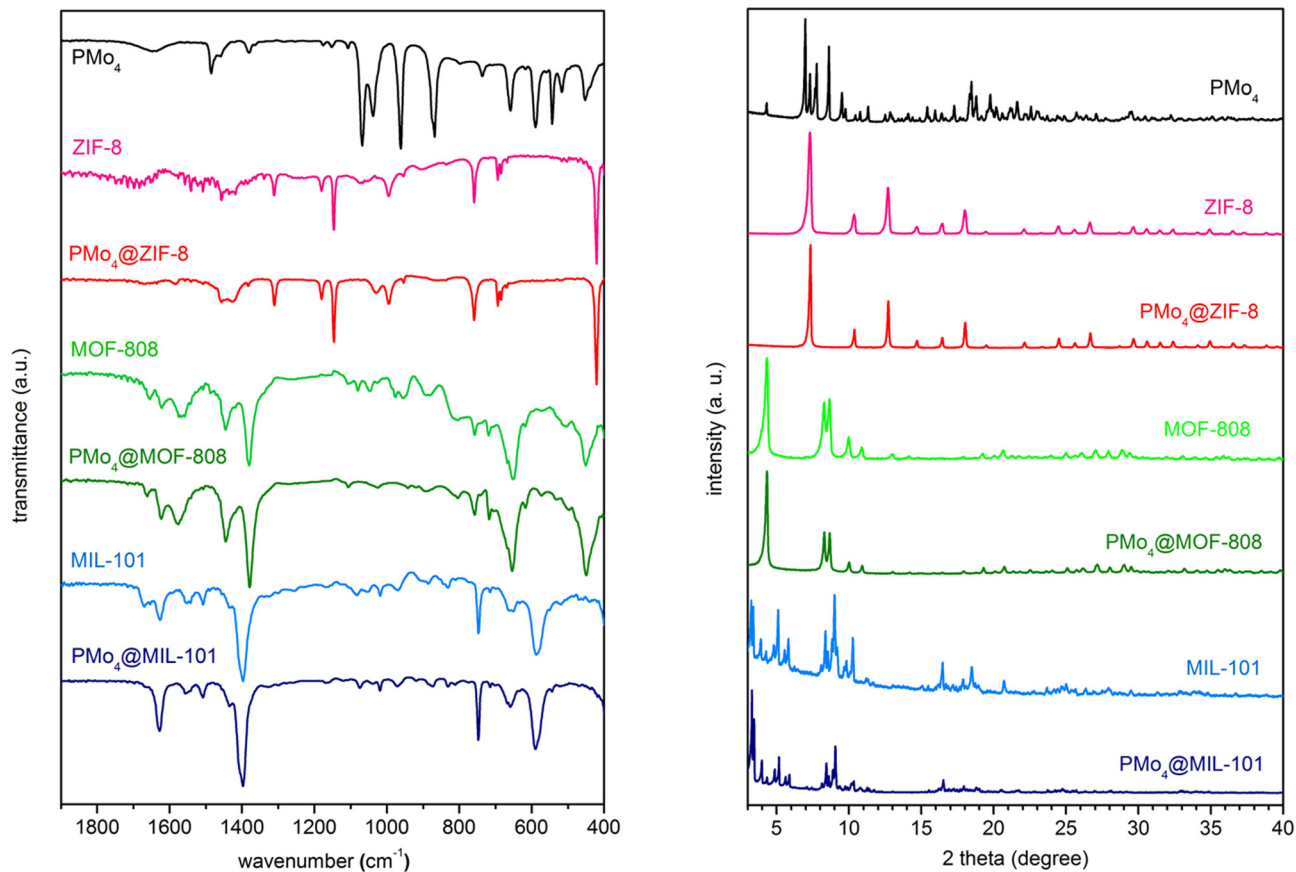
This journal is © The Royal Society of Chemistry 2023

Catal. Sci. Technol., 2023, **13**, 4785–4801 | **4789**

Fig. 1 FT-IR spectra showed in the wavenumber range 1900–400 cm^{-1} (left-hand side) and powder XRD patterns showed between 2 and 40° (right-hand side) from PMo$_4$, pristine MOFs, and PMo$_4$@MOFs composites.

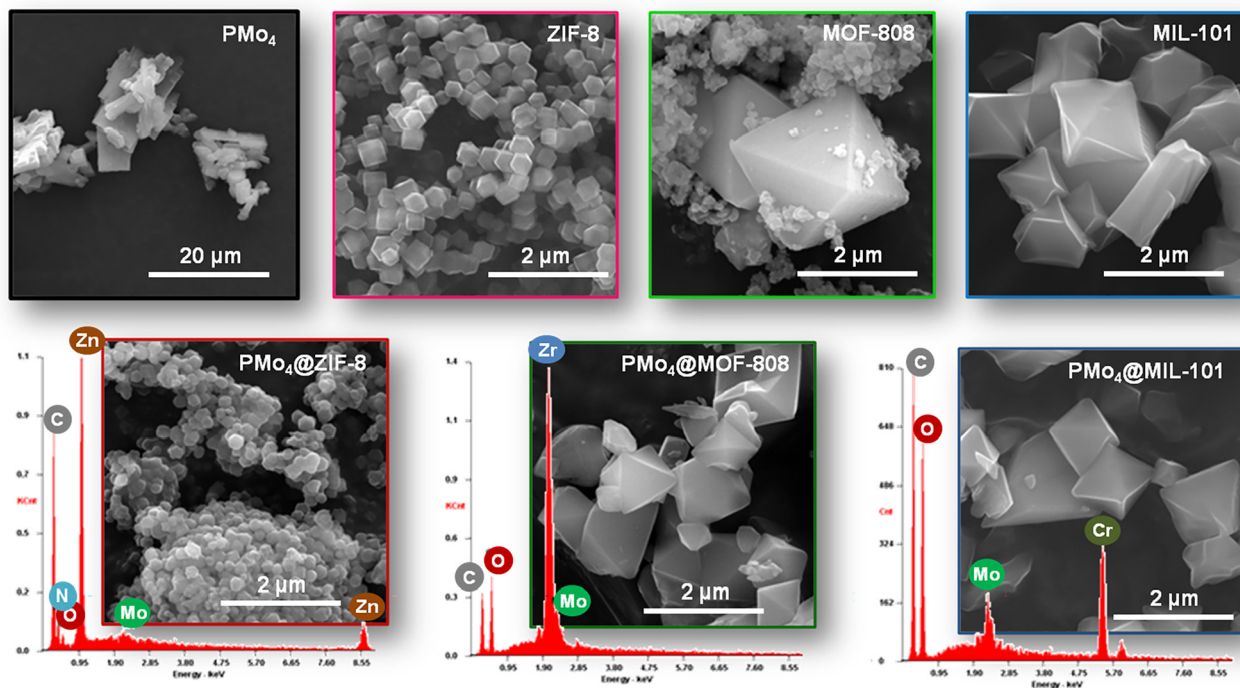**Fig. 2** SEM images of PMo$_4$, the pristine MOFs (ZIF-8, MOF-808, and MIL-101), and the composites (PMo$_4$@ZIF-8, PMo$_4$@MOF-808, and PMo$_4$@MIL-101) overlaid by the corresponding EDX spectra.
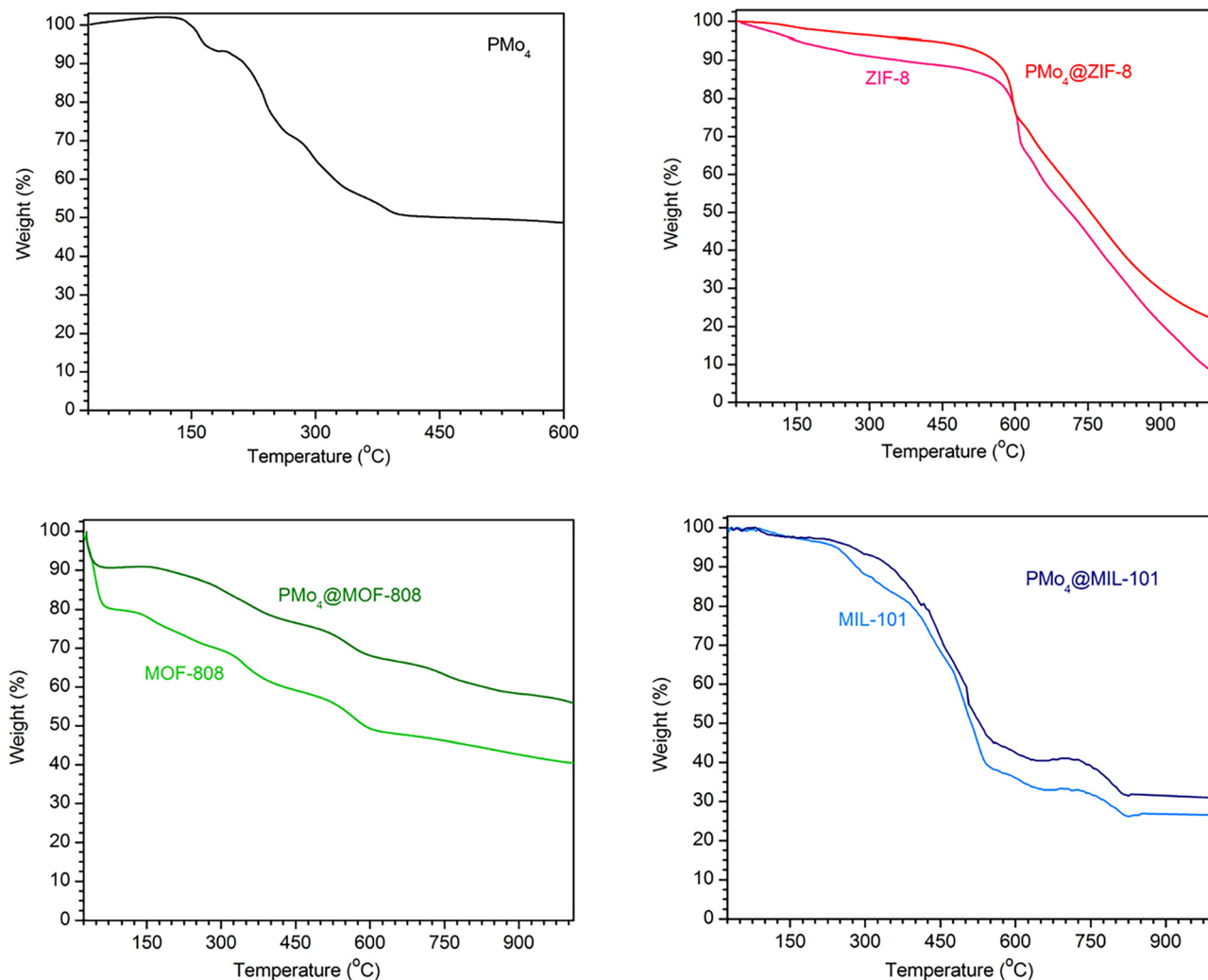
Fig. 3 TGA curves for PMo$_4$ (top left), ZIF-8 and PMo$_4$@ZIF-8 (top right), MOF-808 and PMo$_4$@MOF-808 (bottom left), MIL-101(Cr) and PMo$_4$@MIL-101(Cr) (bottom right).

by four refractory organosulfur compounds (1-BT, DBT, 4-MDBT, and 4,6-DMDBT), combining extraction and catalytic oxidative desulfurization steps (ECODS). The ECODS experiments were performed using biphasic liquid–liquid immiscible phases with equal volumes of the model diesel and the extraction solvent. The homogeneous PMo$_4$ and heterogeneous PMo$_4$@MOFs catalysts were tested using H$_2$O$_2$ as an oxidant at 70 °C (Scheme 3). The influence of using different extraction solvents (MeCN; the ionic liquid, *i.e.*, [BMIM]PF$_6$; and the deep eutectic solvent, *i.e.*, TBACl/PEG) was investigated. The ECODS process consisted of two steps: extraction of sulfur compounds from diesel to the extraction phase and subsequent catalytic oxidation in the extraction phase. Initially, biphasic model diesel and extraction solvent were thoroughly stirred for 10 min to extract part of the sulfur compounds from the diesel phase to the polar extraction solvent phase. After this time, the extraction of the sulfur compounds reached an equilibrium, and the oxidative catalytic step was initiated by the addition of aqueous H$_2$O$_2$ (0.26 mmol) as the oxidant. When the sulfur compounds

were oxidized, more sulfur components were transferred from diesel to the extraction phase (Scheme 3).

3.2.1. Optimization of the ECODS process. The influence of various parameters in the ECODS process was studied to improve total desulfurization efficiency. These include the nature of the extraction solvent, amount of catalyst, and oxidizing H$_2$O$_2$. This optimization study was performed at 70 °C, using PMo$_4$ as a homogeneous catalyst. The reaction temperature was previously optimized using the peroxomolybdate/H$_2$O$_2$ ECODS system.[38]

To investigate the influence of different extraction solvents on the oxidative catalytic performance and sulfur extraction efficiency, acetonitrile, the ionic liquid, *i.e.*, [BMIM]PF$_6$, and the deep eutectic liquid, *i.e.*, TBACl/PEG, were used and the results are displayed in Fig. 5a. From the results obtained using the homogeneous catalyst, PMo$_4$, it could be verified that all three solvents resulted in a similar initial extraction obtained after 10 min, which indicated a similar extractive desulfurization efficiency (around 50%). However, distinct oxidative catalytic desulfurization was achieved after the first
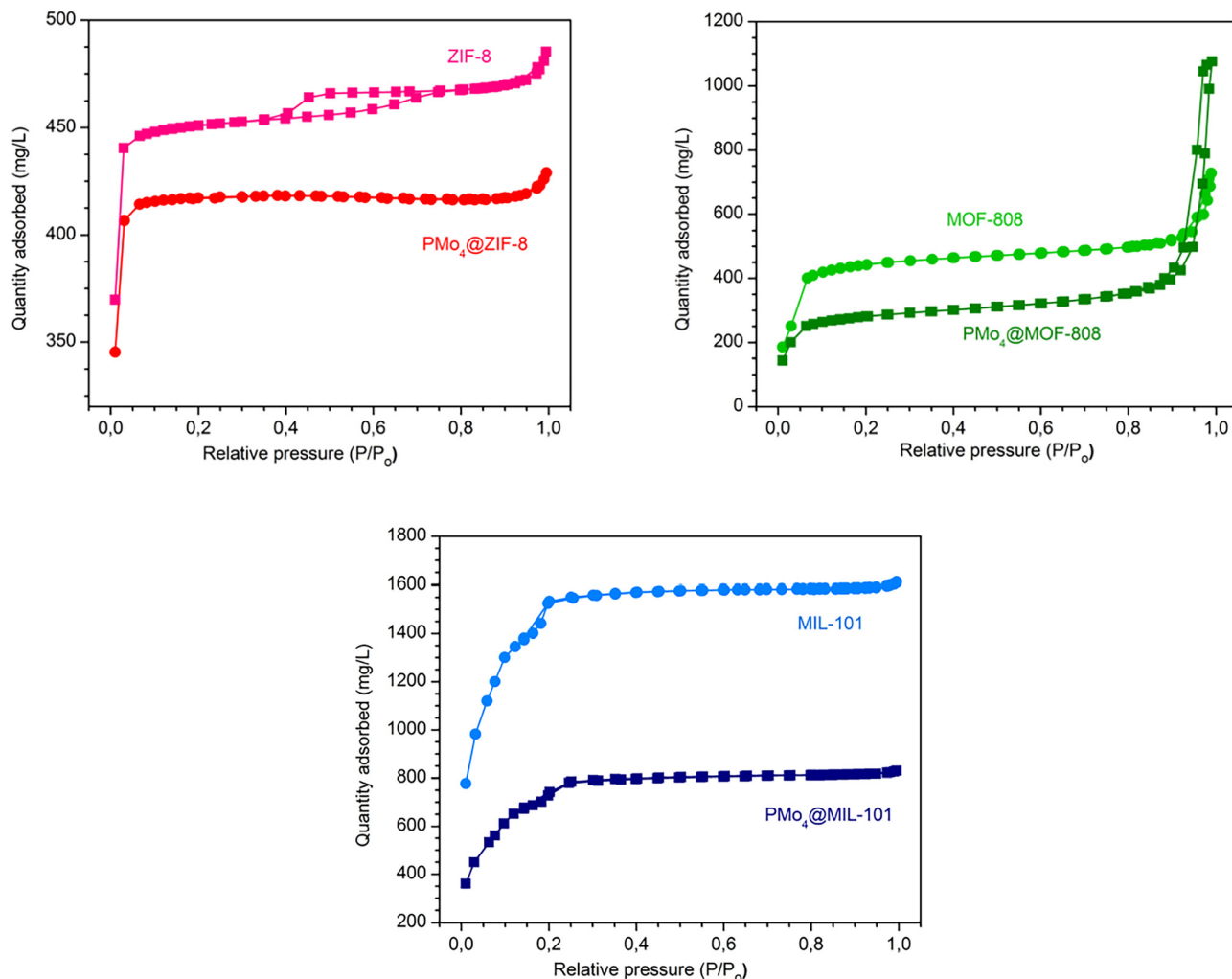
Fig. 4 Nitrogen adsorption–desorption isotherms at −196 °C for MOFs and the corresponding PMo₄@MOFs composites.

10 min, where the highest desulfurization efficiency was found using the ionic liquid, [BMIM]PF$_6$, and TBACl/PEG (66.8% after 2 h). These last extraction solvents presented similar desulfurization profiles. Using acetonitrile, the desulfurization practically stopped after initial extraction only, as only 2.4% of oxidative desulfurization resulted during the catalytic step after 2 h. This means that this solvent did not promote the catalytic activity of the PMo₄
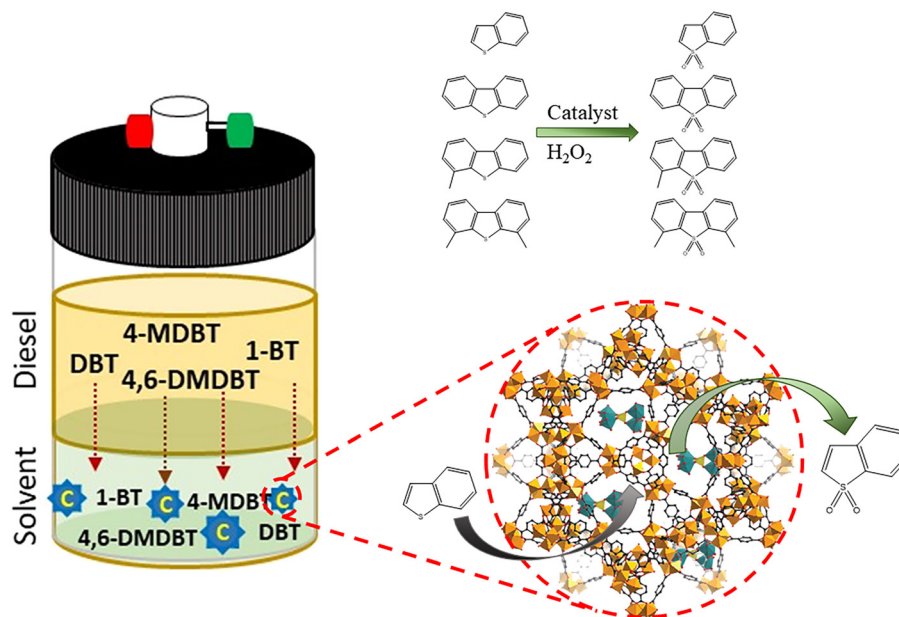
Table 1 The specific surface area of pristine MOFs and corresponding PMo₄@MOFs

Sample	Specific surface area (m² g⁻¹)
ZIF-8	1242
PMo₄@ZIF-8	846
MOF-808	1375
PMo₄@MOF-808	885
MIL-101	4861
PMo₄@MIL-101	2479

catalyst. These results are consistent with the results reported in our previous work.[64] To further verify the superiority of the two-phase liquid system, a solvent-free contrast experiment was conducted under the same conditions as previously described. In this case, the desulfurization resulted only from the catalytic oxidation of sulfur compounds in the model diesel phase, which were then easily removed from the less polar phase (using, for example, acetonitrile). Considering the catalytic step alone, the system was able to remove ~38% of sulfur from model diesel after 2 h of reaction. As previously reported by our group, the catalytic activity of these types of hybrid POMs under solvent-free conditions is strongly influenced by the type of cation.[76]

The influence of the amount of oxidant on the desulfurization efficiency was addressed using [BMIM]PF$_6$ as an extraction solvent (Fig. 5b). The results showed a significant positive effect on the desulfurization performance with increasing H$_2$O$_2$ amount. For an H$_2$O$_2$ dosage of 0.78 mmol, the total desulfurization rapidly increased to a maximum of 98.9% during the first hour of the reaction.

4792 | *Catal. Sci. Technol.*, 2023, **13**, 4785–4801

This journal is © The Royal Society of Chemistry 2023

Scheme 3 Illustration of the ECODS processes using heterogeneous PMo₄@MOFs catalysts.

However, with 1.04 mmol of H_2O_2, the efficiency was similar to that recorded with 0.78 mmol of H_2O_2. This result must be related to the introduction of an excess of aqueous solution (since the oxidant is 30% H_2O_2 in the aqueous phase) into the system that could have hindered the sulfur transfer from the model diesel to the extraction phase. Therefore, the amount of H_2O_2 should be reduced as much as possible under the premise of high efficiency and cost-effectiveness.

The Venturello peroxomolybdate contains active oxygen atoms that are capable of transferring oxygen to sulfur compounds. However, in the next step, the peroxo structure must be re-generated by the interaction of H_2O_2 oxidant *via* hydroxyl radicals formation, making the amount of H_2O_2 an important parameter for catalyst efficiency as suggested previously in the literature on the analogous peroxotungstate PW_4.[64,77]

The effect of PMo_4 amount was also studied to perform the desulfurization of model diesel using the optimized amount of H_2O_2 (0.78 mmol) and $[BMIM]PF_6$ solvent. As shown in Fig. 5c, with the increase in PMo_4 amount, the catalytic activity (after the initial 10 min) sharply increased up to the highest value and then remained constant. Practically complete desulfurization was achieved (99.4%) after the first hour using 7.5 μmol of PMo_4.

Fig. 5d presents the individual removal efficiency of each organosulfur compound catalyzed by a homogeneous PMo_4 catalyst under the optimized reaction parameters (0.78 mmol of H_2O_2, 7.5 μmol of PMo_4, and $[BMIM]PF_6$ as extraction solvent). During the initial extraction stage, the extraction capacity of the four sulfur components followed the order: 1-BT > DBT > 4-MDBT > 4,6-DMDBT, which is mainly correlated to the molecular size and the sulfur atom electronic density as previously described.[30,78–80] Both the electron density and steric hindrance of sulfur atoms affect

the efficiency of sulfur oxidation. The lower electron density of sulfur in 1-BT (5.739) results in the lowest activity for its oxidation. DBT, 4-MDBT, and 4,6-DMDBT possess similar electron densities around the sulfur atom, namely 5.758, 5.759, and 5.760, respectively, resulting in similar final desulfurization efficiency.[80] Nevertheless, the steric hindrance caused by the methyl substituents in 4-MDBT and 4,6-DMDBT makes the oxidation of sulfur more difficult than in DBT.[80]

3.2.2. Stability of the PMo_4/$[BMIM]PF_6$ system. Due to the high solubility of the Venturello PMo_4 catalyst in the $[BMIM]PF_6$ extraction solvent, it cannot be removed and isolated from the ECODS system, but its stability was investigated by reusing the PMo_4/$[BMIM]PF_6$ extraction phase for 10 consecutive desulfurization cycles. Therefore, the desulfurized model diesel at the end of each cycle was separated from the extraction phase containing the soluble active catalytic center. In the next step, a fresh untreated model diesel (0.75 mL) and the oxidant H_2O_2 (0.78 mmol) were added to start a new ECODS cycle (Fig. 6). The results show that the sulfur removal performance of the PMo_4/$[BMIM]PF_6$ system was nearly constant for 10 ECODS cycles (always higher than 91%). The remarkable performance of the system allowed the removal of 94.2% of the sulfur from model diesel even at the end of the 10th consecutive cycle with the same initial portion of extraction solvent. These results indicate that no loss of homogeneous PMo_4 occurred during the reuse process, and the visual accumulation of oxidized products in the extraction phase did not decrease the desulfurization efficiency of the PMo_4/$[BMIM]PF_6$ ECODS system.

3.2.3. Desulfurization using heterogeneous PMo_4@MOFs. The heterogeneous catalysts were prepared by a strategic encapsulation of the active PMo_4 in three different porous MOF frameworks (MIL-101, MOF-808, and ZIF-8). These
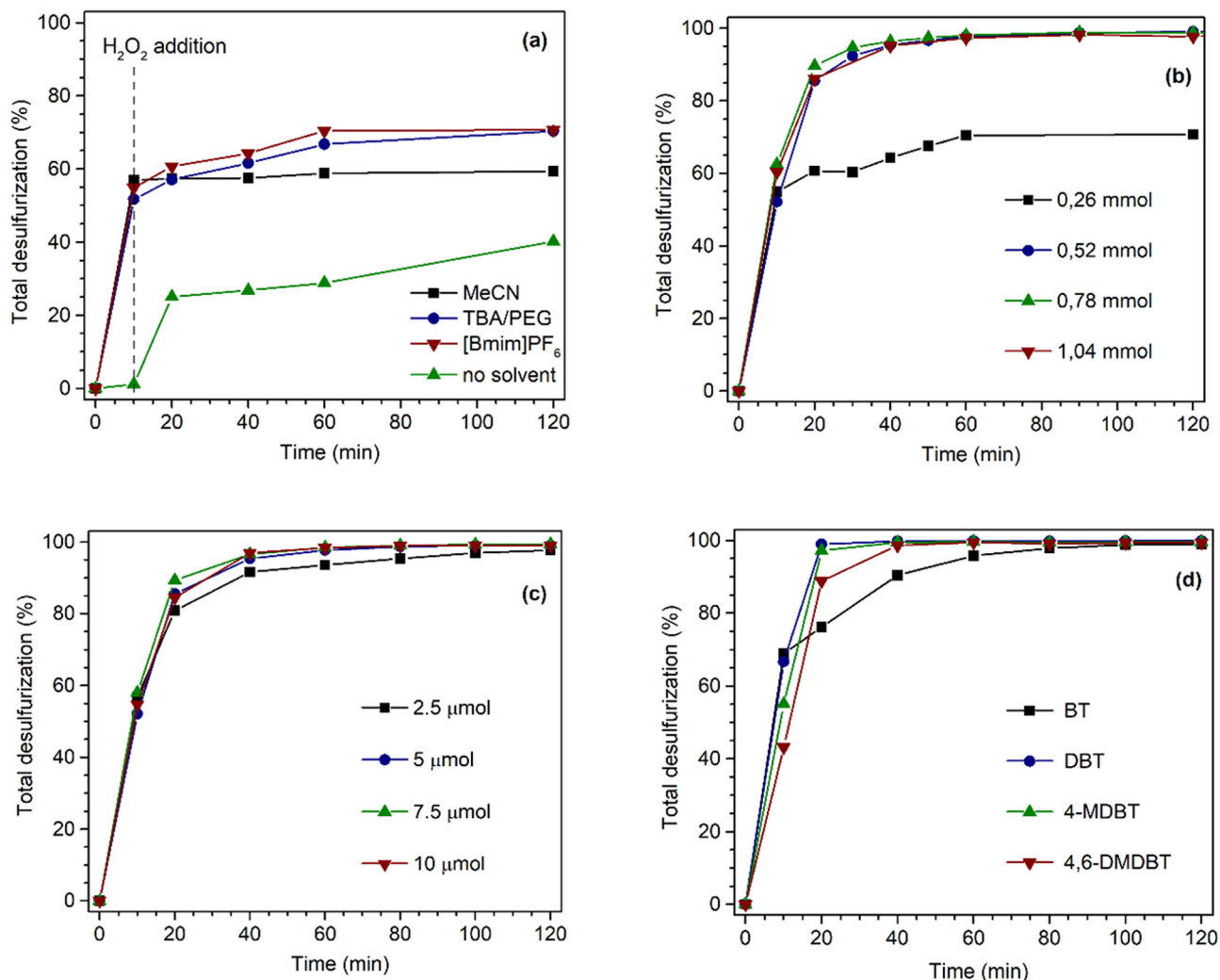
This journal is © The Royal Society of Chemistry 2023

Catal. Sci. Technol., 2023, **13**, 4785–4801 | **4793**

Fig. 5 Desulfurization profile of a multicomponent model diesel (2000 ppm of S) catalyzed by the homogeneous PMo_4 (5 μmol) and in the presence of different extraction solvents (0.75 mL) using 0.26 mmol H_2O_2 at 70 °C (a); the effect of the amount of H_2O_2 on oxidative desulfurization in the presence of [BMIM]PF_6 (0.75 mL) using 5 μmol of PMo_4 at 70 °C (b); the effect of the amount of PMo_4 on oxidative desulfurization in the presence of [BMIM]PF_6 (0.75 mL) using 0.78 mmol of H_2O_2 at 70 °C (c); and the desulfurization efficiency of each sulfur compound in the presence of [BMIM]PF_6 (0.75 mL) using 0.78 mmol of H_2O_2 and 7.5 μmol of PMo_4 at 70 °C (d).

Fig. 6 Reusability of the homogeneous PMo_4 (7.5 μmol) catalyst using 0.75 mL of [BMIM]PF_6 extraction solvent, 0.78 mmol of H_2O_2, and 7.5 μmol of PMo_4 at 70 °C. The results were obtained at 2 h.

heterogeneous catalysts were tested to desulfurize the multicomponent model diesel under the previously optimized conditions. The influence of the nature of the support on the catalytic performance of the active center was evaluated. Catalytic performance and the recycling capacity of the composite PMo_4@MOF must be directly correlated to its structural properties, *i.e.*, to the nature of the ligands and the metallic centers, as well as its cage and window sizes. Fig. 7a displays the desulfurization results obtained using the various heterogeneous PMo_4@MOFs catalysts. After 2 h, the desulfurization obtained using PMo_4@MIL-101, PMo_4@MOF-808, and PMo_4@ZIF-8 were 99.2; 73.1, and 68.1%, respectively. The most efficient catalyst was the one that presented the highest cage cavity and window entrance sizes. The window size of PMo_4@MIL-101 (*ca.* 12–16 Å^2) was larger than the molecular size of any of the sulfur substrates, which

4794 | *Catal. Sci. Technol.*, 2023, **13**, 4785–4801

This journal is © The Royal Society of Chemistry 2023

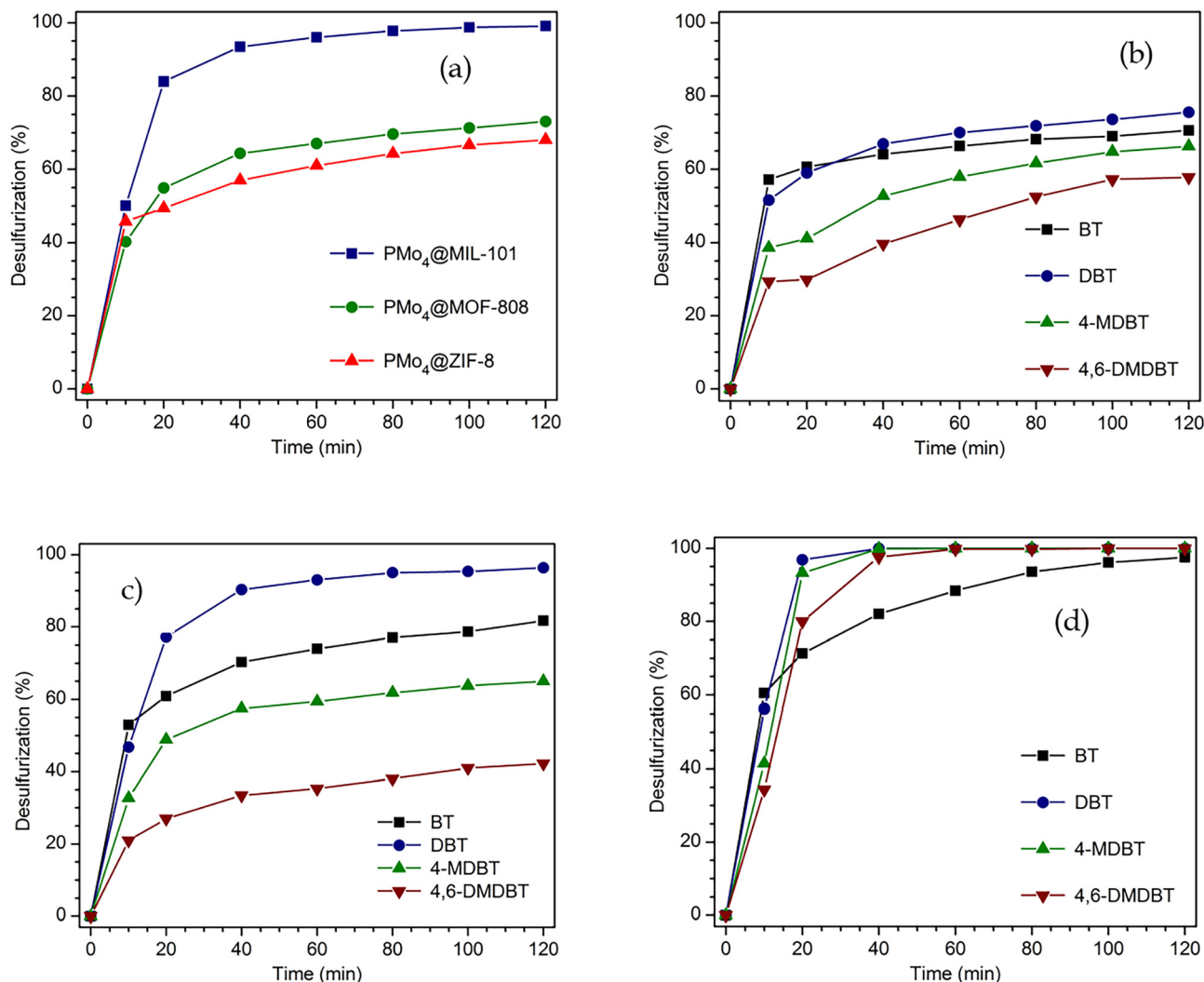**Fig. 7** Desulfurization profile of the multicomponent model diesel (2000 ppm of S) catalyzed by PMo$_4$@MOFs, containing 7.5 µmol PMo$_4$ with 0.75 mL of [BMIM]PF$_6$ as the extraction solvent and 0.78 mmol H$_2$O$_2$ at 70 °C (a). Desulfurization profile of each sulfur compound present in the model diesel catalyzed by PMo$_4$@ZIF-8 (b), PMo$_4$@MOF-808 (c), and PMo$_4$@MIL-101 (d).

could help facilitate the diffusion of the reactants into the MOF cages, accelerating the reaction and leading to higher efficiency. The narrow window of ZIF-8 (*ca.* 3.4 × 3.4 Å^2) might constrain access of the sulfur substrates into the MOF cavities, leading to the lowest activity. Interestingly, the overall desulfurization ability of the four sulfur substrates during the process catalyzed by PMo$_4$@MIL-101 still followed the same trend as that described previously for the homogeneous PMo$_4$ system: DBT > 4-MDBT > 4,6-DMDBT > BT. In contrast, the removal ability of the sulfur compounds for the PMo$_4$@MOF-808 and PMo$_4$@ZIF-8 systems followed the order: DBT > BT > 4-MDBT > 4,6-DMDBT (Fig. 7b and c), revealing a clear relationship between the window size of the porous framework and the molecular size of the sulfur substrates. Indeed, the narrower window sizes limit the diffusion of the larger 4-MDBT and 4,6-DMDBT molecules, while the small-sized 1-BT compounds can still be diffused into the porous cavities. Moreover, in the case of

PMo$_4$@ZIF-8, the extremely narrow windows of ZIF-8 may also hinder the diffusion of DBT as seen by its considerably lower desulfurization percentage (72% after 2 h, Fig. 7b). Therefore, a direct relationship between the sulfur molecule size and the cavity entrance size was found here, which may indicate that the active catalytic center is accessible only in the cages of MOF frameworks.

The high catalytic efficiency of the PMo$_4$@MIL-101 heterogeneous catalyst motivated recycling studies on it. The catalyst was evaluated for 10 consecutive cycles using [BMIM]PF$_6$ as extraction solvent under optimized conditions (Fig. 8). At the end of each ECODS cycle, the solid catalyst was recovered by centrifugation, washed with MeCN, and dried. It was then used in the next cycle, while maintaining the experimental conditions. Furthermore, the PMo$_4$@MIL-101/[BMIM]PF$_6$ system was reused and, in this case, only the desulfurized model diesel was removed from the system at the end of each cycle. Afterward, new portions of fresh
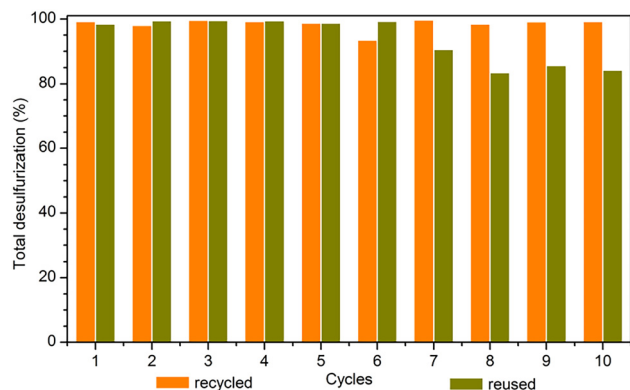
Fig. 8 Recyclability and reusability of ECODS system using the PMo$_4$@MIL-101 catalyst under the optimized conditions (catalyst containing 7.5 μmol of PMo$_4$, 0.75 mL of extraction solvent [BMIM]PF$_6$, and 0.78 mmol of H$_2$O$_2$ at 70 $^\circ$C). Results were obtained after 2 h.

untreated model diesel and oxidant were added to the remaining [BMIM]PF$_6$ phase containing the solid catalyst to start the next ECODS cycle. As depicted in Fig. 8, this PMo$_4$@MIL-101 composite showed remarkable stability and high recyclability during the 10 consecutive catalytic cycles without apparent reduction in its desulfurization performance. The results of the reusability studies show a reduction in the desulfurization ability after the 7th cycle. This is probably due to the continuous accumulation of oxidized products (precipitated sulfones) in the extraction layer, making the extraction of raw sulfides increasingly difficult. However, it is noteworthy that the reuse of the PMo$_4$@MIL-101-catalyzed system could still remove 99.3% of the sulfur at the end of the 6th cycle, especially considering the continuous reuse of the initial volume of extraction solvent.

3.2.4. Comparison with other reported catalysts. Reports on the use of immobilized peroxopolyoxometalates as heterogeneous catalysts for desulfurization processes are scarce and absent in the case of peroxopolyoxomolybdate. Few examples can be found in the literature for the immobilization of the peroxopolyoxotungstate compound, $\{PO_4[WO(O_2)_2]_4\}^{3-}$ (PW$_4$), on the surface of a functionalized mesoporous SBA-15 support[40] and also its encapsulation in a MOF structure with larger pore cavities, such as MIL-101(Cr),[80,81] and smaller cavities, such as UiO-66.[81] Complete desulfurization of

multicomponent sulfur model fuel has been observed using these peroxotungstate-based composites (Table 2). The first work was published in 2019 by Julião *et al.*, when PW$_4$ was immobilized on a propyltrimethylammonium (TMA)-functionalized SBA-15.[40] Using this PW$_4$@TMA-SBA-15 catalyst, complete desulfurization was achieved after 2 h using acetonitrile as the extraction solvent. Faster complete desulfurization of similar multi-component model fuels was achieved using porous metal–organic frameworks as the support material for the active center, PW$_4$.[2,82] Three different works have reported the use of [BMIM]PF$_6$ ionic liquid as extraction solvent, and complete desulfurization was achieved after approximately 1 h. In this work, peroxomolybdate was used instead of the reported peroxotungstate. In this case, similar desulfurization efficiency was achieved using MIL-101 as the support material; however, in this work a simple procedure was followed to prepare PMo$_4$@MIL-101-based solid catalyst, obtaining even a higher reutilization and recycling capacity than PW$_4$@MIL-101 in consecutive reaction cycles.[81]

3.3. Catalyst stability

The recovered PMo$_4$@MIL-101 catalyst after being used for 10 consecutive ECODS cycles was characterized by various techniques. The FT-IR spectra and powder XRD patterns of PMo$_4$@MIL-101 after recycling and reusing displayed profiles similar to the ones of fresh PMo$_4$@MIL-101, suggesting that the structure of the composite was preserved during the continuous 10 catalytic cycles (Fig. 9a and b). Nonetheless, some additional FT-IR bands could be observed after catalytic use, mainly for reused PMo$_4$@MIL-101, in the 1300–1000 and 550–450 cm^{-1} ranges. The morphology of recycled and reused catalysts retained the typical octahedral shape of the original material with no evidence of degradation having occurred (Fig. 9c and d). Small heteromorphic particles were detected in the reused catalyst, which correspond to some precipitated sulfones that remained adsorbed on the surface of the catalyst even after washing, as has been reported previously for different catalytic materials used in oxidative desulfurization.[80] The previously described additional bands in the FT-IR spectrum of reused PMo$_4$@MIL-101 can also be assigned to the presence of such adsorbed oxidized sulfides in the catalyst. From all of the above observations, the characterization data after catalytic use revealed that the

Table 2 Comparison of catalytic efficiency of heterogeneous peroxopolyoxometalate catalysts for desulfurization of multi-component model fuels (containing 1-BT, DBT, 4-MDBT, and 4,6-DMDBT) at 70 $^\circ$C

Catalyst	Time (h)	Solvent	Efficiency (%)	Ref.
PW$_4$@TMA-SBA-15	2	MeCN	100	40
PW$_4$@MIL-101	0.7	[BMIM]PF$_6$	99	2
PW$_4$@Fe$_2$O$_3$/MIL-101	1	[BMIM]PF$_6$	99	77
PW$_4$@UiO-66-NH$_2$	1	[BMIM]PF$_6$	99	82
PMo$_4$@MIL-101	1	[BMIM]PF$_6$	97	This work
PMo$_4$@MOF-808	1	[BMIM]PF$_6$	69	This work
PMo$_4$@ZIF-8	1	[BMIM]PF$_6$	63	This work

4796 | *Catal. Sci. Technol.*, 2023, **13**, 4785–4801
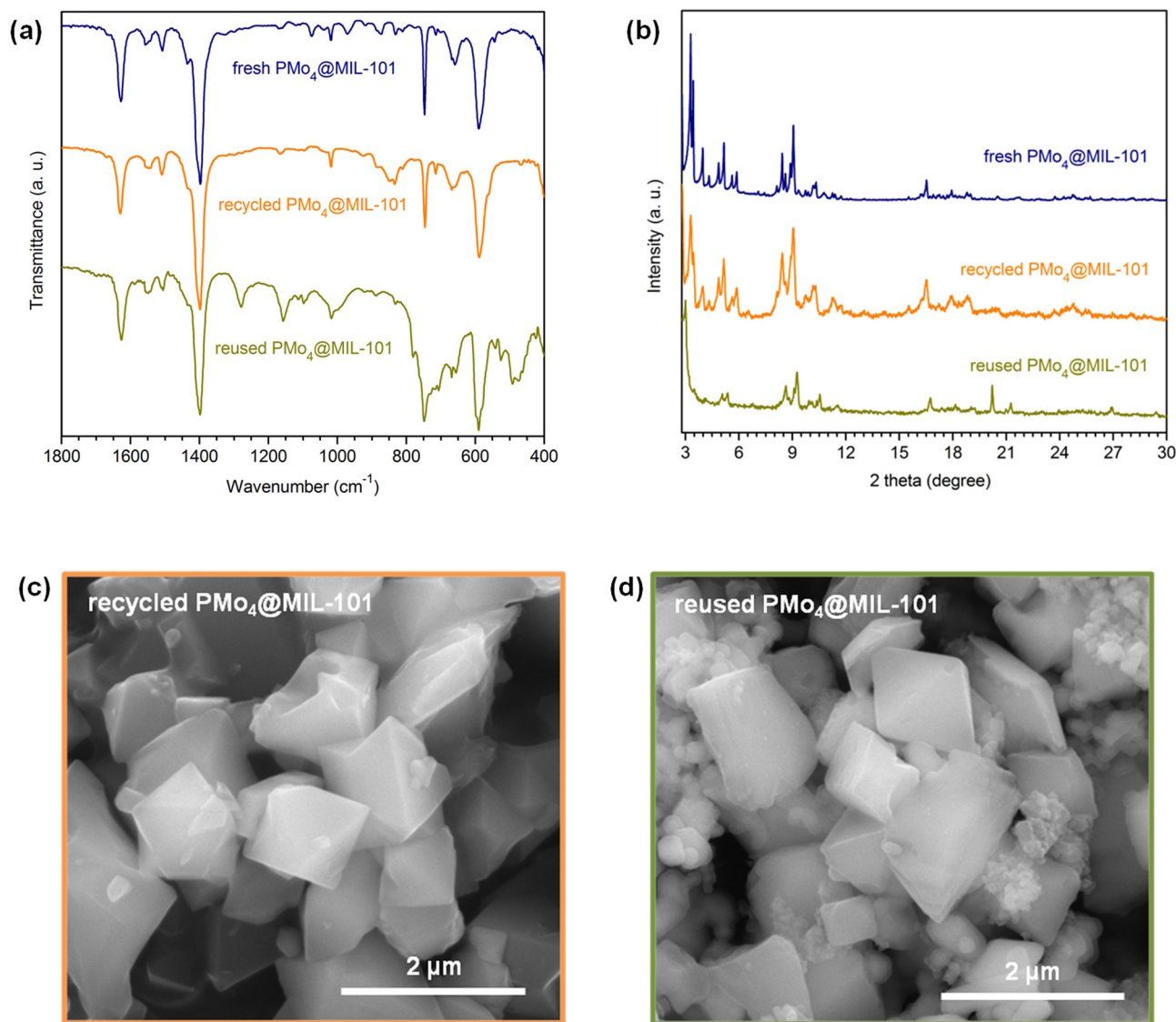
This journal is © The Royal Society of Chemistry 2023

Fig. 9 Characterization data obtained for fresh, recycled, and reused PMo$_4$@MIL-101 heterogeneous catalysts: FT-IR spectra (a), powder XRD patterns (b), and SEM images (c and d).

PMo$_4$@MIL-101 composite shows outstanding stability during the high-efficiency ECODS process.

4. Conclusions

The active TBA$_3$\{PO$_4$[MoO(O$_2$)$_2$]$_4$\} (PMo$_4$) compound was successfully used in the desulfurization of a multicomponent model diesel and its homogeneous and heterogeneous performance was compared. The heterogenization of PMo$_4$ was performed by its immobilization in different MOF supports. These presented distinct windows and cage cavity sizes (PMo$_4$@MIL-101, PMo$_4$@MOF-808, and PMo$_4$@ZIF-8). Effective incorporation of PMo$_4$ was achieved by following strategic procedures according to the MOF structural properties. The three prepared composites were characterized fully by several techniques, and the catalytic performance of the materials was tested. Optimization of the reaction

conditions was performed using the PMo$_4$ as the active catalytic center, resulting in total desulfurization after only 2 h using the [BMIM]PF$_6$ ionic liquid as extraction solvent. Optimized conditions were applied to study the catalytic efficiency of PMo$_4$@MOFs. The highest catalytic performance was found for PMo$_4$@MIL-101, achieving near-complete desulfurization after 2 h. A significantly lower catalytic performance was obtained for PMo$_4$@MOF-808 and PMo$_4$@ZIF-8 (73.1 and 68.1%, respectively). Since the same amount of active center was used, the higher catalytic performance of the MIL-101 composite must be related to its higher window entrance and cavity sizes that promote a higher diffusion of molecules to the MIL-101 cavities and allow higher accessibility to the active catalytic centers. The PMo$_4$@MIL-101 catalyst presented the highest activity associated with a high recycle capacity (10 reaction cycles without activity loss) and structural stability. Following the

This journal is © The Royal Society of Chemistry 2023

Catal. Sci. Technol., 2023, **13**, 4785–4801 | **4797**

remarkable physicochemical properties and desulfurization efficiency exhibited by the PMo_4@MIL-101 catalyst, further work will be developed to desulfurize real untreated fuel samples, such as diesel and heavy fuel oils.

Conflicts of interest

There are no conflicts to declare.

Acknowledgements

References

1 F. Johnsson, J. Kjärstad and J. Rootzén, The threat to climate change mitigation posed by the abundance of fossil fuels, *Clim. Policy*, 2019, **19**, 258–274.

2 Y. Gao, F. Mirante, B. de Castro, J. Zhao, L. Cunha-Silva and S. S. Balula, An Effective Hybrid Heterogeneous Catalyst to Desulfurize Diesel: Peroxotungstate@Metal–Organic Framework, *Molecules*, 2020, **25**, 5494.

3 M. E. Luvsan, R. H. Shie, T. Purevdorj, L. Badarch and C. C. Chan, The influence of emission sources and meteorological conditions on SO_2 pollution in Mongolia (vol 61C, pg 542, 2012), *Atmos. Environ.*, 2012, **61**, 542–549.

4 A. Hamidi, S. M. Mirsalim and P. Sharghi, Optimum blend of biodiesel ultra-low sulfur in order to improve lubrication and achieve Euro 5 standard, in *The 8th International Conference on Internal Combustion Engines and Oil*, 2014.

5 Marine fuels: Price impact of new 2020 low sulfur regulations negated by refineries and Covid-19, *Oil and Energy Trends*, 2020, vol. 45, pp. 3–5.

6 J. W. Rich, Method for producing ultra clean liquid fuel from coal refuse, *US Pat.*, US6869979B1, 2005.

7 M. Silk, M. Ackiewicz, J. Anderson and O. Ogunsola, Overview of Fundamentals of Synthetic Ultraclean Transportation Fuel Production, *EMBO J.*, 2001, **20**, 6060–6070.

8 I. V. Babich and J. A. Moulijn, Science and technology of novel processes for deep desulfurization of oil refinery streams: A review, *Fuel*, 2003, **82**, 607–631.

9 S. A. Ganiyu and S. A. Lateef, Review of adsorptive desulfurization process: Overview of the non-carbonaceous materials, mechanism and synthesis strategies, *Fuel*, 2021, **294**, 120273.

10 S. Tahir, U. Y. Qazi, Z. Naseem, N. Tahir, M. Zahid, R. Javaid and I. Shahid, Deep eutectic solvents as alternative green solvents for the efficient desulfurization of liquid fuel: A comprehensive review, *Fuel*, 2021, **305**, 121502.

11 T. Zhang, J. T. Zhang, Z. Wang, J. H. Liu, G. Y. Qian, D. Wang and X. Z. Gong, Review of electrochemical oxidation desulfurization for fuels and minerals, *Fuel*, 2021, **305**, 121562.

12 A. Haruna, Z. M. A. Merican and S. G. Musa, Recent advances in catalytic oxidative desulfurization of fuel oil-A review, *J. Ind. Eng. Chem.*, 2022, **112**, 20–36.

13 M. S. Nazir, S. Ahmad, Z. Tahir, S. U. Hassan, Z. Ali, M. N. Akhtar, K. Azam and M. A. Abdullah, A Review on the Methods in Diesel Desulfurization, *Curr. Anal. Chem.*, 2021, **17**, 815–830.

14 L. Sun, T. Su, J. Xu, D. Hao, W. Liao, Y. Zhao, W. Ren, C. Deng and H. Lü, Aerobic oxidative desulfurization coupling of Co polyanion catalysts and p-TsOH-based deep eutectic solvents through a biomimetic approach, *Green Chem.*, 2019, 2629–2634.

15 M. Adhami, S. Movahedirad and M. A. Sobati, Oxidative desulfurization of fuels using gaseous oxidants: a review, *J. Sulfur Chem.*, 2022, **46**(6), 685–712.

16 M. Ahmadian and M. Anbia, Oxidative Desulfurization of Liquid Fuels Using Polyoxometalate-Based Catalysts: A Review, *Energy Fuels*, 2021, **35**, 10347–10373.

17 A. T. Albayrak and A. Tavman, Sono-oxidative desulfurization of fuels using heterogeneous and homogeneous catalysts: A comprehensive review, *Ultrason. Sonochem.*, 2022, **83**, 105845.

18 F. Boshagh, M. Rahmani, K. Rostami and M. Yousefifar, Key Factors Affecting the Development of Oxidative Desulfurization of Liquid Fuels: A Critical Review, *Energy Fuels*, 2022, **36**, 98–132.

19 F. F. Roman, J. L. D. de Tuesta, A. M. T. Silva, J. L. Faria and H. T. Gomes, Carbon-Based Materials for Oxidative Desulfurization and Denitrogenation of Fuels: A Review, *Catalysts*, 2021, **11**, 1239.

20 A. Tanimu, G. Tanimu, S. A. Ganiyu, Y. Gambo, H. Alasiri and K. Alhooshani, Metal-Free Catalytic Oxidative Desulfurization of Fuels-A Review, *Energy Fuels*, 2022, **36**, 3394–3419.

21 B. Yuan, X. L. Li and Y. Y. Sun, A Short Review of Aerobic Oxidative Desulfurization of Liquid Fuels over Porous Materials, *Catalysts*, 2022, **12**, 129.

22 M. N. Hossain, H. C. Park and H. S. Choi, A Comprehensive Review on Catalytic Oxidative Desulfurization of Liquid Fuel Oil, *Catalysts*, 2019, **9**, 229.

23 S. Houda, C. Lancelot, P. Blanchard, L. Poinel and C. Lamonier, Oxidative Desulfurization of Heavy Oils with High Sulfur Content: A Review, *Catalysts*, 2018, **8**, 344.

24 F. Liu, J. Yu, A. B. Qazi, L. Zhang and X. K. Liu, Metal-Based Ionic Liquids in Oxidative Desulfurization: A Critical Review, *Environ. Sci. Technol.*, 2021, **55**, 1419–1435.

25 A. Rajendran, T. Y. Cui, H. X. Fan, Z. F. Yang, J. Feng and W. Y. Li, A comprehensive review on oxidative desulfurization catalysts targeting clean energy and environment, *J. Mater. Chem. A*, 2020, **8**, 2246–2285.

4798 | *Catal. Sci. Technol.*, 2023, **13**, 4785–4801

This journal is © The Royal Society of Chemistry 2023

26 A. K. Sharipov and V. R. Nigmatullin, Oxidative desulfurization of diesel fuel (a review), *Pet. Chem.*, 2005, **45**, 371–377.

27 M. Taghizadeh, E. Mehrvarz and A. Taghipour, Polyoxometalate as an effective catalyst for the oxidative desulfurization of liquid fuels: a critical review, *Rev. Chem. Eng.*, 2020, **36**, 831–858.

28 N. F. Nejad, E. Shams and M. K. Amini, Ionic Liquid-based Extraction of Sulfur Compounds From Gasoline as a Complementary Process to Oxidative Desulfurization, *Pet. Sci. Technol.*, 2014, **32**, 1537–1544.

29 N. Abas, A. Kalair and N. Khan, Review of fossil fuels and future energy technologies, *Futures*, 2015, **69**, 31–49.

30 S. O. Ribeiro, C. M. Granadeiro, P. L. Almeida, J. Pires, M. C. Capel-Sanchez, J. M. Campos-Martin, S. Gago, B. de Castro and S. S. Balula, Oxidative desulfurization strategies using Keggin-type polyoxometalate catalysts: Biphasic versus solvent-free systems, *Catal. Today*, 2019, **333**, 226–236.

31 S. O. Ribeiro, L. S. Nogueira, S. Gago, P. L. Almeida, M. C. Corvo, B. de Castro, C. M. Granadeiro and S. S. Balula, Desulfurization process conciliating heterogeneous oxidation and liquid extraction: Organic solvent or centrifugation/water?, *Appl. Catal., A*, 2017, **542**, 359–367.

32 W. Jiang, H. Jia, H. P. Li, L. H. Zhu, R. M. Tao, W. S. Zhu, H. M. Li and S. Dai, Boric acid-based ternary deep eutectic solvent for extraction and oxidative desulfurization of diesel fuel, *Green Chem.*, 2019, **21**, 3074–3080.

33 J. M. Campos-Martin, M. C. Capel-Sanchez, P. Perez-Presas and J. L. G. Fierro, Oxidative processes of desulfurization of liquid fuels, *J. Chem. Technol. Biotechnol.*, 2010, **85**, 879–890.

34 C. M. Granadeiro, A. D. S. Barbosa, S. Ribeiro, I. Santos, B. de Castro, L. Cunha-Silva and S. S. Balula, Oxidative catalytic versatility of a trivacant polyoxotungstate incorporated into MIL-101(Cr), *Catal. Sci. Technol.*, 2014, **4**, 1416–1425.

35 C. M. Granadeiro, P. M. C. Ferreira, D. Juliao, L. A. Ribeiro, R. Valenca, J. C. Ribeiro, I. S. Goncalves, B. de Castro, M. Pillinger, L. Cunha-Silva and S. S. Balula, Efficient Oxidative Desulfurization Processes Using Polyoxomolybdate Based Catalysts, *Energies*, 2018, **11**, 1696.

36 C. M. Granadeiro, L. S. Nogueira, D. Juliao, F. Mirante, D. Ananias, S. S. Balula and L. Cunha-Silva, Influence of a porous MOF support on the catalytic performance of Eu-polyoxometalate based materials: desulfurization of a model diesel, *Catal. Sci. Technol.*, 2016, **6**, 1515–1522.

37 C. M. Granadeiro, S. O. Ribeiro, M. Karmaoui, R. Valenca, J. C. Ribeiro, B. de Castro, L. Cunha-Silva and S. S. Balula, Production of ultra-deep sulfur-free diesels using a sustainable catalytic system based on UiO-66(Zr), *Chem. Commun.*, 2015, **51**, 13818–13821.

38 D. Juliao, A. C. Gomes, L. Cunha-Silva, R. Valenca, J. C. Ribeiro, M. Pillinger, B. de Castro, I. S. Goncalves and S. S. Balula, A sustainable peroxophosphomolybdate/H_2O_2 system for the oxidative removal of organosulfur compounds from simulated and real high-sulfur diesels, *Appl. Catal., A*, 2020, **589**, 117154.

39 D. Juliao, A. C. Gomes, M. Pillinger, L. Cunha-Silva, B. de Castro, I. S. Goncalves and S. S. Balula, Desulfurization of model diesel by extraction/oxidation using a zinc-substituted polyoxometalate as catalyst under homogeneous and heterogeneous (MIL-101 (Cr) encapsulated) conditions, *Fuel Process. Technol.*, 2015, **131**, 78–86.

40 D. Julião, F. Mirante, S. O. Ribeiro, A. C. Gomes, R. Valença, J. C. Ribeiro, M. Pillinger, B. de Castro, I. S. Gonçalves and S. S. Balula, Deep oxidative desulfurization of diesel fuels using homogeneous and SBA-15-supported peroxophosphotungstate catalysts, *Fuel*, 2019, **241**, 616–624.

41 C. Streb, K. Kastner and J. Tucher, Polyoxometalates in photocatalysis, *Asia Pac. J. Risk. Insur.*, 2019, **4**, 105–121.

42 D. C. Bao, L. C. Dou, D. M. Ren, Y. Zhao and Y. S. Xia, Review in catalytic oxidation desulfurization by polyoxometalates, *Bohai Daxue Xuebao, Ziran Kexueban*, 2017, **3**, 211–217.

43 D. C. Duncan, R. C. Chambers, E. Hecht and C. L. Hill, Mechanism and dynamics in the $H_3PW_{12}O_{40}$ – catalyzed selective epoxidation of terminal olefins by H_2O_2. Formation, reactivity, and stability of $\{PO_4[WO(O_2)_2]_4\}^{3-}$, *J. Am. Chem. Soc.*, 1995, **117**, 681–691.

44 J. R. Li, Z. Yang, S. W. Li, Q. P. Jin and J. S. Zhao, Review on oxidative desulfurization of fuel by supported heteropolyacid catalysts, *J. Ind. Eng. Chem.*, 2020, **82**, 1–16.

45 J. J. Stracke and R. G. Finke, Distinguishing Homogeneous from Heterogeneous Water Oxidation Catalysis when Beginning with Polyoxometalates, *ACS Catal.*, 2014, **4**, 909–933.

46 W. Xie and H. Wang, Synthesis of heterogenized polyoxometalate-based ionic liquids with Brönsted-Lewis acid sites: A magnetically recyclable catalyst for biodiesel production from low-quality oils, *J. Ind. Eng. Chem.*, 2020, **87**, 162–172.

47 W. Xie, C. Gao and J. Li, Sustainable biodiesel production from low-quantity oils utilizing $H_6PV_3MoW_8O_{40}$ supported on magnetic Fe_3O_4/ZIF-8 composites, *Renewable Energy*, 2021, **168**, 927–937.

48 K. Maru, S. Kalla and R. Jangir, MOF/POM hybrids as catalysts for organic transformations, *Dalton Trans.*, 2022, **51**, 11952–11986.

49 P. Mialane, C. Mellot-Draznieks, P. Gairola, M. Duguet, Y. Benseghir, O. Oms and A. Dolbecq, Heterogenisation of polyoxometalates and other metal-based complexes in metal-organic frameworks: from synthesis to characterisation and applications in catalysis, *Chem. Soc. Rev.*, 2021, **50**, 6152–6220.

50 W. Xie and J. Li, Magnetic solid catalysts for sustainable and cleaner biodiesel production: A comprehensive review, *Renewable Sustainable Energy Rev.*, 2023, **171**, 113017.

51 D. Y. Du, J. S. Qin, S. L. Li, Z. M. Su and Y. Q. Lan, Recent advances in porous polyoxometalate-based metal-organic framework materials, *Chem. Soc. Rev.*, 2014, **43**, 4615–4632.

52 J. M. Sun, S. Abednatanzi, P. Van Der Voort, Y. Y. Liu and K. Leus, POM@MOF Hybrids: Synthesis and Applications, *Catalysts*, 2020, **10**, 578.

53 S. W. Zhang, F. X. Ou, S. G. Ning and P. Cheng, Polyoxometalate-based metal-organic frameworks for heterogeneous catalysis, *Inorg. Chem. Front.*, 2021, **8**, 1865–1899.

This journal is © The Royal Society of Chemistry 2023

Catal. Sci. Technol., 2023, **13**, 4785–4801 | 4799

54 R. Abazari, L. Esrafili, A. Morsali, Y. H. Wu and J. K. Gao, PMo_{12}@UiO-67 nanocomposite as a novel non-leaching catalyst with enhanced performance durability for sulfur removal from liquid fuels with exceptionally diluted oxidant, *Appl. Catal., B*, 2021, **283**, 119582.

55 S. C. Fernandes, A. M. Viana, B. de Castro, L. Cunha-Silva and S. S. Balula, Synergistic combination of the nanoporous system of MOF-808 with a polyoxomolybdate to design an effective catalyst: simultaneous oxidative desulfurization and denitrogenation processes, *Sustainable Energy Fuels*, 2021, **5**, 4032–4040.

56 Y. K. Lu, C. L. Yue, B. X. Liu, M. Zhang, Y. P. Li, W. F. Yang, Y. Lin, Y. Pan, D. F. Sun and Y. Q. Liu, The encapsulation of POM clusters into MIL-101(Cr) at molecular level: $LaW_{10}O_{36}$@MIL-101(Cr), an efficient catalyst for oxidative desulfurization, *Microporous Mesoporous Mater.*, 2021, **311**, 110694.

57 P. P. Wei, Y. Yang, W. Z. Li and G. M. Li, Keggin-POM@rht-MOF-1 composite as heterogeneous catalysts towards ultra-deep oxidative fuel desulfurization, *Fuel*, 2020, **274**, 117834.

58 W. L. Xie and F. Wan, Immobilization of polyoxometalate-based sulfonated ionic liquids on UiO-66-2COOH metal-organic frameworks for biodiesel production via one-pot transesterification-esterification of acidic vegetable oils, *Chem. Eng. J.*, 2019, **365**, 40–50.

59 N. Yang, L. J. Lu, L. H. Zhu, P. W. Wu, D. J. Tao, X. W. Li, J. H. Gong, L. L. Chen, Y. H. Chao and W. S. Zhu, Phosphomolybdic acid encapsulated in ZIF-8-based porous ionic liquids for reactive extraction desulfurization of fuels, *Inorg. Chem. Front.*, 2022, **9**, 165–178.

60 G. Ye, L. L. Hu, Y. L. Gu, C. Lancelot, A. Rives, C. Lamonier, N. Nuns, M. Marinova, W. Xu and Y. Y. Sun, Synthesis of polyoxometalate encapsulated in UiO-66(Zr) with hierarchical porosity and double active sites for oxidation desulfurization of fuel oil at room temperature, *J. Mater. Chem. A*, 2020, **8**, 19396–19404.

61 S. Fernandes, D. Flores, D. Silva, I. Santos-Vieira, F. Mirante, C. M. Granadeiro and S. S. Balula, Lindqvist@Nanoporous MOF-Based Catalyst for Effective Desulfurization of Fuels, *Nanomaterials*, 2022, **12**, 2887.

62 D. F. Silva, A. M. Viana, I. Santos-Vieira, S. S. Balula and L. Cunha-Silva, Ionic Liquid-Based Polyoxometalate Incorporated at ZIF-8: A Sustainable Catalyst to Combine Desulfurization and Denitrogenation Processes, *Molecules*, 2022, **27**, 1711.

63 Y. Zhang and R. Wang, Synthesis of silica@C-dots/phosphotungstates core-shell microsphere for effective oxidative-adsorptive desulfurization of dibenzothiophene with less oxidant, *Appl. Catal., B*, 2018, **234**, 247–259.

64 Y. Gao, D. Julião, D. F. Silva, B. de Castro, J. S. Zhao and S. S. Balula, A simple desulfurization process to achieve high efficiency, sustainability and cost-effectivity via peroxotungstate catalyst, *Mol. Catal.*, 2021, **505**, 111515.

65 Z. Y. Qi, Z. X. Huang, H. X. Wang, L. Li, C. S. Ye and T. Qiu, In situ bridging encapsulation of a carboxyl-functionalized phosphotungstic acid ionic liquid in UiO-66: A remarkable catalyst for oxidative desulfurization, *Chem. Eng. Sci.*, 2020, **225**, 115818.

66 Z. Y. Qi, H. F. Li, J. Chen, C. S. Ye and T. Qiu, Intensification of oxidative desulfurization by Zr(IV)-ionic liquid-HPW composite activating H_2O_2 system and mechanism insight, *Fuel*, 2022, **322**, 124231.

67 M. Ghahramaninezhad, F. Pakdel and M. N. Shahrak, Boosting oxidative desulfurization of model fuel by POM-grafting ZIF-8 as a novel and efficient catalyst, *Polyhedron*, 2019, **170**, 364–372.

68 X. Sang, G. Shi, N. I. Caihua and D. Wang, Zr-MOFs as catalysts for the N-acylation of ethyl acetate, *Huagong Jinzhan*, 2019, 3311–3318.

69 C. M. Granadeiro, A. D. S. Barbosa, P. Silva, F. A. A. Paz, V. K. Saini, J. Pires, B. de Castro, S. S. Balula and L. Cunha-Silva, Monovacant polyoxometalates incorporated into MIL-101(Cr): novel heterogeneous catalysts for liquid phase oxidation, *Appl. Catal., A*, 2013, **453**, 316–326.

70 A. Jomekian, B. Bazooyar, R. M. Behbahani, T. Mohammadi and A. Kargari, Ionic liquid-modified Pebax 1657 membrane filled by ZIF-8 particles for separation of CO_2 from CH_4, N_2 and H_2, *J. Membr. Sci.*, 2017, **524**, 652–662.

71 J. Xu, L. Jin, L. Zhen, X. Wang, Y. Xu, S. Chen and W. Zhuo, Optimized synthesis of Zr(IV) metal organic frameworks (MOFs-808) for efficient hydrogen storage, *New J. Chem.*, 2019, **43**, 4092–4099.

72 A. Mansoor and H. Vahid, Enhancement of CO_2 adsorption on nanoporous chromium terephthalate (MIL-101) by amine modification, *J. Nat. Gas Chem.*, 2012, **21**(3), 339–343.

73 J. Feng, Y. Zhong, M. Xie, M. Li and S. Jiang, Using MOF-808 as a Promising Support to Immobilize Ru for Selective Hydrogenation of Levulinic Acid to γ-Valerolactone, *Catal. Lett.*, 2021, **151**, 86–94.

74 J. Cravillon, S. Münzer, S.-J. Lohmeier, A. Feldhoff, K. Huber and M. Wiebcke, Rapid Room-Temperature Synthesis and Characterization of Nanocrystals of a Prototypical Zeolitic Imidazolate Framework, *Chem. Mater.*, 2009, **21**, 1410–1412.

75 J. Pires, M. L. Pinto, C. M. Granadeiro, A. D. S. Barbosa, L. Cunha-Silva, S. S. Balula and V. K. Saini, Effect on selective adsorption of ethane and ethylene of the polyoxometalates impregnation in the metal-organic framework MIL-101, *Adsorption*, 2014, **20**, 533–543.

76 F. Mirante, B. de Castro, C. M. Granadeiro and S. S. Balula, Solvent-Free Desulfurization System to Produce Low-Sulfur Diesel Using Hybrid Monovacant Keggin-Type Catalyst, *Molecules*, 2020, **25**, 4961.

77 Y. Gao, M. Yan, L. T. Chen and J. S. Zhao, Encapsulated peroxophosphotungstates catalyst into magnetic MOF: Magnetically recoverable heterogeneous high efficiency desulfurization catalyst, *J. Environ. Chem. Eng.*, 2022, **10**, 108270.

78 F. Mirante, L. Dias, M. Silva, S. O. Ribeiro, M. C. Corvo, B. de Castro, C. M. Granadeiro and S. S. Balula, Efficient heterogeneous polyoxometalate-hybrid catalysts for the oxidative desulfurization of fuels, *Catal. Commun.*, 2018, **104**, 1–8.

4800 | *Catal. Sci. Technol.*, 2023, **13**, 4785–4801

This journal is © The Royal Society of Chemistry 2023

79 S. O. Ribeiro, C. M. Granadeiro, P. L. Almeida, J. Pires, R. Valença, J. M. Campos-Martin, J. C. Ribeiro, B. de Castro and S. S. Balula, Effective Zinc-Substituted Keggin Composite To Catalyze the Removal of Sulfur from Real Diesels under a Solvent-Free System, *Ind. Eng. Chem. Res.*, 2019, **58**, 18540–18549.

80 S. O. Ribeiro, L. S. Nogueira, S. Gago, P. L. Almeida, M. C. Corvo, B. de Castro, C. M. Granadeiro and S. S. Balula, Desulfurization process conciliating heterogeneous oxidation and liquid extraction: Organic solvent or centrifugation/water?, *Appl. Catal., A*, 2017, **542**, 359–367.

81 C. M. Granadeiro, L. S. Nogueira, D. Julião, F. Mirante, D. Ananias, S. S. Balula and L. Cunha-Silva, Influence of a porous MOF support on the catalytic performance of Eu-polyoxometalate based materials: desulfurization of a model diesel, *Catal. Sci. Technol.*, 2016, **6**, 1515–1522.

82 Y. Gao, M. Yan and J. S. Zhao, Metal-organic framework (UIO-66-NH$_2$)-encapsulated peroxophosphotungstate (PW$_4$) loaded on graphene oxide (GO) as catalyst for desulfurization of fuel, *Microporous Mesoporous Mater.*, 2022, **341**, 112105.

This journal is © The Royal Society of Chemistry 2023

Catal. Sci. Technol., 2023, **13**, 4785–4801 | **4801**